

## RF Sputtered MoO<sub>3</sub> Thin Film on Si (100) for Gas Sensing Applications

Akhilesh Pandey<sup>@,\*</sup>, Anoushka Dhaka<sup>#</sup>, Chandni Kumari<sup>§</sup>, Janesh Kaushik<sup>@</sup>, Aman Arora<sup>@</sup>,  
Shankar Dutta<sup>@</sup>, Ambesh Dixit<sup>§</sup>, and R. Raman<sup>@</sup>

<sup>@</sup>DRDO-Solid State Physics Laboratory, Delhi - 110 054, India

<sup>#</sup>Punjab Engineering College, Chandigarh - 160 012, India

<sup>§</sup>Indian Institute of Technology, Jodhpur - 342 037, India

\*E-mail: [akhilesh.physics@gmail.com](mailto:akhilesh.physics@gmail.com)

### ABSTRACT

Molybdenum Trioxide (MoO<sub>3</sub>) films are grown on Si(100) substrates by reactive RF magnetron sputtering in plasma containing a mixture of Argon and Oxygen, using a pure Molybdenum target. In this paper, we report the deposition of (MoO<sub>3</sub>) films on Si(100) substrates under varying gas flow (O<sub>2</sub> + Ar gas) (20 sccm to 30 sccm with the duration of deposition ~ 1hr) by RF reactive magnetron sputtering at room temperature. To get crystalline MoO<sub>3</sub> films annealing in O<sub>2</sub> environment at 500 °C for 4 h is done. Phase formation and orientation of the film is characterised by Glancing incidence X-ray diffraction (GIXRD). The identification of the orthorhombic MoO<sub>3</sub> phase is investigated by XRD and Raman spectroscopy. Raman lines at 819 cm<sup>-1</sup> and 995 cm<sup>-1</sup> are due to the (A<sub>1g</sub>, B<sub>1g</sub>) symmetric stretching (Mo–O–Mo) bond and asymmetric stretching band (Mo=O) respectively. Surface morphology and cross-sectional image of the deposited thin films were investigated by FE-SEM image. UV-Visible reflectance and cross-sectional FE-SEM image confirm the thickness of the MoO<sub>3</sub> films with oxygen-rich and oxygen deficient phase formation occur. Reverse leakage current density of 20 sccm 1hr sample is low (1×10<sup>-6</sup> mA/cm<sup>2</sup>) as compared to 30 sccm 1hr sample (1×10<sup>-3</sup> mA/cm<sup>2</sup>). The higher leakage is due to crack formation during the ex-situ annealing of MoO<sub>3</sub> films. This MoO<sub>3</sub> films can be used in Gas sensing and switching devices.

**Keywords:** MoO<sub>3</sub>; Sputtering; XRD; Reflectance; FESEM; Leakage current; Gas sensing

### 1. INTRODUCTION

Among the transition metal oxides, Molybdenum oxide (MoO<sub>3</sub>) is one of the most potential materials for the variety of technological applications such as large-scale electrochromic devices, coatings for optical switching and memory devices<sup>1</sup>. MoO<sub>3</sub> is intensively used for sensing various gases like NO<sub>2</sub>, NH<sub>3</sub>, Ethanol, Methanol, H<sub>2</sub> and H<sub>2</sub>S gases<sup>2</sup> and various volatile organic compounds (VOC)<sup>3</sup>. The thin films of MoO<sub>3</sub> can also be used in solar cells, micro-batteries, supercapacitors etc<sup>4-5</sup>.

MoO<sub>3</sub> is a wide bandgap semiconductor of bandgap approximately 3.3 eV. Usually, MoO<sub>3</sub> gets crystallised in two different phases<sup>6</sup>. Orthorhombic,  $\alpha$ -MoO<sub>3</sub>, which is the most stable phase and the other one, is a metastable monoclinic  $\beta$ -MoO<sub>3</sub> crystal phase. MoO<sub>3</sub> has good chemical stability and as-deposited films normally have amorphous structure which on annealing at 300 °C crystallizes to the monoclinic phase and above 400 °C to 600 °C, it crystallizes orthorhombic  $\alpha$ -MoO<sub>3</sub> phase.

MoO<sub>3</sub> thin films can be prepared by different growth techniques like sputtering<sup>7-8</sup>, molecular beam epitaxy<sup>9</sup>, pulsed laser deposition<sup>10-11</sup>, atomic layer deposition<sup>12</sup>, chemical vapor deposition<sup>13</sup>, spray pyrolysis<sup>14</sup> and sol-gel<sup>15</sup>. Among them, sputtering is more preferred for the deposition of high quality

of MoO<sub>3</sub> films due to ease in operation and effective in cost. The commonly used substrate for MoO<sub>3</sub> thin films are Glass, Quartz, Si and GaAs.

Sarkar<sup>6</sup>, *et al.* have studied the interface study of MoO<sub>3</sub> thin films on GaAs substrate for Solar cell applications. Arfaoui<sup>16</sup>, *et al.* have studied the structural and morphological properties MoO<sub>3</sub> and WO<sub>3</sub> thin films prepared by thermal evaporation for gas sensing and photocatalytic applications. Touihri<sup>17</sup>, *et al.* studied the annealing effect of MoO<sub>3</sub> films and found the multiphase of MoO<sub>3</sub> films.

Researchers have identified the MoO<sub>3</sub> multiphase usually by XRD and Raman analysis<sup>18-19</sup> but proper analysis of ex-situ annealed RF sputtered MoO<sub>3</sub> films by structural, optical and electrical analysis to identify the multiphase with oxygen deficiency or oxygen-rich in MoO<sub>3</sub> films are less studied. Therefore in this study it is planned to grow the MoO<sub>3</sub> thin films by RF sputtering by varying the oxygen pressure. After growing the film its annealing effect under oxygen environment has studied using structural, optical and electrical characterisations.

This paper discusses the deposition of MoO<sub>3</sub> thin films on Si (100) substrate by RF sputtering technique (with Mo target) at different oxygen partial pressure and thereafter ex-situ annealed at 500 °C. The phase and microstructure of the annealed samples are reported. The optical and electrical properties of the MoO<sub>3</sub> films are also reported.

## 2. EXPERIMENTAL TECHNIQUES

The two MoO<sub>3</sub> films were deposited using RF reactive magnetron sputtering on Si (100) substrate by varying the oxygen + Ar flow (10 sccm+10 sccm) to (15 sccm+ 15sccm)), together with same deposition time (~1 h) and are named as sample S1 and S2 respectively. After deposition ex-situ annealing was done in O<sub>2</sub> environment at 500 °C for 240 min. The structural evolution together with microstructural and optical properties of MoO<sub>3</sub> thin films was studied using X-ray Diffraction (XRD), Raman spectroscopy, UV-visible reflectance and Field Emission Scanning Electron Microscopy (FE-SEM) measurements. X-ray diffractogram of the MoO<sub>3</sub> films were measured in thin-film geometry using glancing incidence x-ray diffraction (GIXRD) technique. In this geometry x-ray incidence angle ( $\alpha$ ) is kept constant around ~2° from the sample surface. In the diffracted arm. A diffracted signal was detected by the detector by scanning with 2theta angle from 10° to 75° to record the diffractogram. In XRD using Cu K $\alpha$  radiation PANalytical X-Pert Pro MRD HRXRD system is used for phase and orientation parameter analysis. The surface morphology of the films and their cross-section were examined by FE-SEM ( Carl Zeiss Model: SUPRA-50). Raman spectroscopy experiments were performed in the backscattering geometry at room temperature by the confocal Micro-Raman spectrometer system (Model Horiba Jobin Yuvan LABRAM HR Evolution) using frequency-doubled NdYAG laser at 532.15 nm excitation with cooled UV enhanced CCD detector. UV-visible reflectance measurements were done by Agilent make UV-visible spectrophotometer from 200 nm to 850 nm. For electrical I-V characteristics have been obtained from -2 V to +10 V using Keithley 2611B source meter.

## 3. RESULTS AND DISCUSSION

The XRD patterns of synthesised films in grazing incidence geometry (GIXRD) are shown in Fig. 1. The MoO<sub>3</sub> films is found to be polycrystalline in nature having orientations along (020), (110), (040), (021), (130), (111), (041), (150), (200), (002), (112), (109), (202) planes corresponding to the 2 $\theta$  angles of 12.68°, 23.33°, 25.65°, 27.32°, 29.45°, 33.81°, 35.65°, 38.8°, 45.78°, 49.11°, 55.25°, 64.91° and 69.73° in XRD diffractogram. In the XRD pattern of samples S1 and

S2 relatively intense (110) and (021) peak is observed as compared to other XRD peaks respectively. The peak position of XRD pattern is very well matched with the  $\alpha$ -orthorhombic phase of MoO<sub>3</sub>. Some unidentified extra XRD peaks were also observed, marked star (\*) in the Fig. 1. These peaks may be oxygen-deficient molybdenum oxide XRD peaks. As shown in figure sample S1 is more oxygen-deficient as compared to sample S2. The average crystallite size determined by Scherer relation is 16 nm and 20 nm for sample S1 and S2 respectively. The degree of crystallinity for sample S1 (~65%) is relatively low as compared to sample S2 (~70%). The film's orientation changes along (021) to (110) directions as oxygen and Ar flow increases (20 sccm to 30 sccm). Texture Coefficient (TC) of the films along (021) for sample S1 and (110) for sample S2 are determined as equation<sup>20, 21</sup> written below

$$TC(\gamma) = \frac{I_{hkl}}{I_{ohkl}} \quad (1)$$

$$= \frac{1}{N} \sum_{i=1}^N \frac{I_{hkl}}{I_{ohkl}}$$

In the above equation the measured intensity from XRD pattern is  $I_{hkl}$  and  $I_o$  is intensity taken from JCPDS data (file No-05-508). N belongs to the number of diffraction peaks. If the texture coefficient value is less than unity for any crystallographic plane, the film orientation is not preferred along that direction. The calculated texture coefficient of sample S1 along (021) plane is 1.7; while sample S2 along (110) plane is 1.2. Texture coefficients of the MoO<sub>3</sub> sample confirm the crystallites are partially oriented along (021) and (110) for sample S1 and S2 respectively.

XRD peak intensity of sample S1 is low as compared to sample S2 and the degree of crystallinity of S2 is higher as compared to S1. It seems after annealing sample 1(20 sccm, 1h) is still oxygen-deficient as compared to S2.

Figure 2 shows the image of the surface and cross-sectional morphology of sample S1 and sample S2 using FESEM. Figures 2(a) and 2(b) shows the FESEM image of annealed MoO<sub>3</sub> films image of 1 hour grown (Ar +O<sub>2</sub> flow ~ 20 sccm) sample S1. The average grain size of the sample S1 shows the variation from 200 nm to 300 nm. Some large and small grains are distributed in MoO<sub>3</sub> films, apart from grain distribution some small cracks were also observed in the films. Large grains may be MoO<sub>3</sub> flakes that are formed during the annealing in oxygen environment. Figure 2(c) shows the surface morphology of sample 2. The grain size is significantly increased in sample 2 (average grain size is around 300-400nm) which is quite large as compared to sample S1. In the sample S2, small cracks become large and the size of the crack ~20 nm. Figures 2(c) and 2(d) show the cross-sectional image of sample S1 and S2 respectively. The thickness of MoO<sub>3</sub> films measured from the cross-sectional FESEM images is 1.54  $\mu$ m and 1.6  $\mu$ m for sample S1 and S2 respectively. Interestingly in Fig. 2(b) two interfaces are observed. One from the top surface of the film up to ~0.45  $\mu$ m with large grain sized (~200-300 nm), another from this interface to substrate interface (~1.1  $\mu$ m) with grain size below 150 nm. The cross-sectional image of sample-2 shows the uniform grain size ~300 nm. The continuous layer

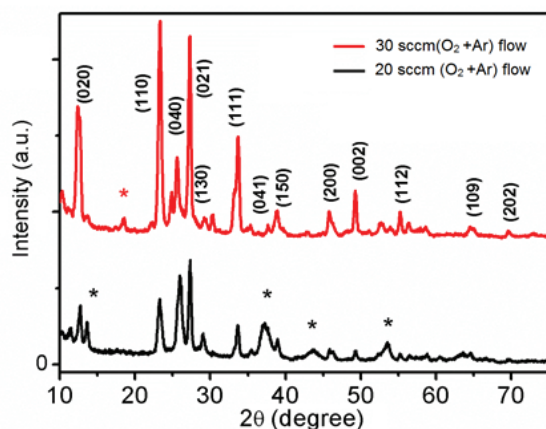
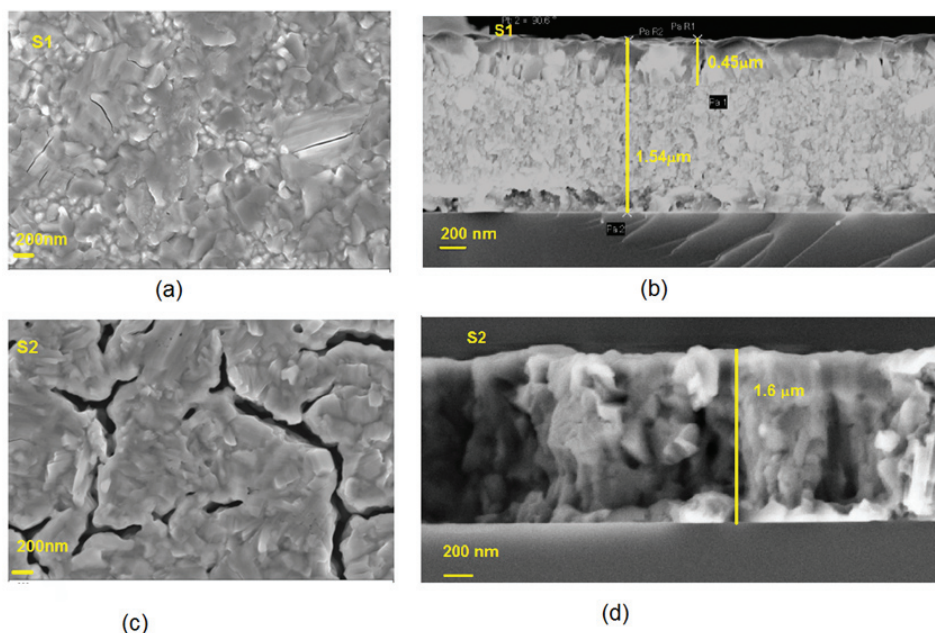


Figure 1. XRD pattern of Annealed MoO<sub>3</sub> films with different O<sub>2</sub> flow.



**Figure 2.** FESEM images of MoO<sub>3</sub> films (a) and (b) planer and cross-sectional for sample S1( 20sccm-1h), (c) and (d) planer and cross-sectional for sample S2( 30sccm-1h).

from the surface of the film to the films-substrate interface is observed with the thickness ( $\sim 1.6 \mu\text{m}$ ).

In the crystalline orthorhombic  $\alpha\text{-MoO}_3$  structures, layers formed by distorted MoO<sub>6</sub> octahedra which are weakly bound by Vander Wall (vdW) forces and all three lattice constants (a, b and c) are different<sup>22,23</sup>. In the unit cell of  $\alpha\text{-MoO}_3$  there exist 16 atoms, four represent molybdenum and others twelve are oxygen. There exist a total 45 phonon modes. The irreducible representation of orthorhombic MoO<sub>3</sub> crystal with the space group (Pbmn) is given by

$$\Gamma = 8A_g + 8B_{1g} + 4B_{2g} + 4B_{3g} + 4A_u + 3B_{1u} + 7B_{2u} + 7B_{3u}$$

where Raman active modes are Ag, B<sub>1g</sub>, B<sub>2g</sub>, and B<sub>3g</sub>. Therefore total 24 phonon modes are Raman active and others (17 Modes = 3B<sub>1u</sub> + 7B<sub>2u</sub> + 7B<sub>3u</sub>) are IR active. Apart from these normal phonon modes 4A<sub>u</sub> are silent. Figure 3 shows the Raman spectra of MoO<sub>3</sub> thin films excited from the green laser. Figure 3 shows the prominent peaks at 118, 152, 199,

218, 247, 280, 338, 367, 382, 472, 660, 819, and 995 cm<sup>-1</sup>, which confirms  $\alpha\text{-MoO}_3$  orthorhombic phase<sup>3</sup>. These Raman active peaks can be indexed with modes: 118 (B<sub>2g</sub>), 129 (B<sub>3g</sub>), 160 (Ag, B<sub>1g</sub>), 199 (B<sub>2g</sub>), 218 (Ag), 247 (B<sub>3g</sub>), 285 (B<sub>2g</sub>, B<sub>3g</sub>), 338 (B<sub>1g</sub>, Ag), 367 (Ag), 382 (B<sub>1g</sub>), 472 (Ag, B<sub>1g</sub>), 667 (B<sub>2g</sub>, B<sub>3g</sub>), 820 (Ag<sub>1</sub>, B<sub>1g</sub>) and 995 (Ag<sub>1</sub>, B<sub>1g</sub>) cm<sup>-1</sup>. The prominent Raman peaks at 819 cm<sup>-1</sup> and 995 cm<sup>-1</sup> are due to the symmetric stretching (Mo=O) band and asymmetric stretching band (Mo=O) respectively. The other Raman lines 667 cm<sup>-1</sup> is the asymmetric stretching band of O-Mo-O, 338 cm<sup>-1</sup> is a bending mode of O-Mo-O and 285 cm<sup>-1</sup> is wagging mode of O=Mo=O. The relative Raman intensity and peak position are almost matching with previously reported MoO<sub>3</sub> Raman modes<sup>22</sup>. Raman peaks are intense and prominent for sample S2 (30 sccm 1hr) as compare to S1. Due to the high degree of crystallinity determined by XRD pattern, Raman intensity of sample S2 (30 sccm 1hr) is more intense as compared to sample S1 (20 sccm 1h).

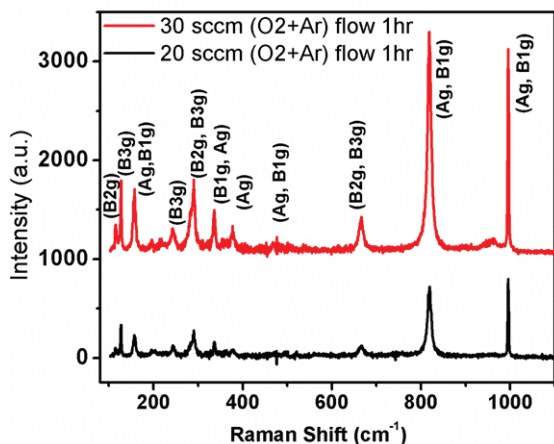


**Figure 3.** Raman spectra of annealed MoO<sub>3</sub> films with different O<sub>2</sub> flow excited by green 532nm LASER.

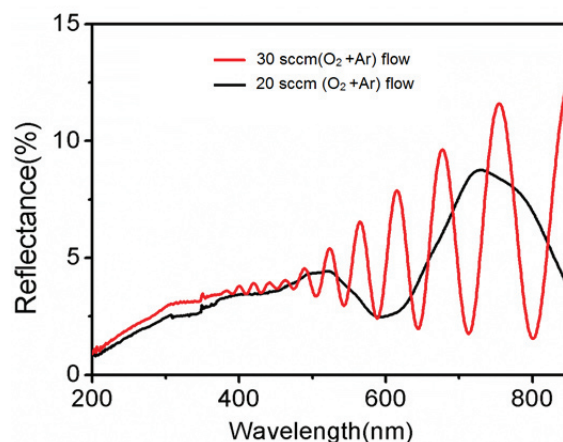


**Figure 4.** UV-Visible reflectance plot of MoO<sub>3</sub> films.



The UV-visible Reflectance measurement of MoO<sub>3</sub> films grown on Si (100) substrates is done at room temperature. Due to the low bandgap of Si substrates as compare to MoO<sub>3</sub>, the transmittance study for samples 1 and 2 is not possible in the UV-visible range, Therefore reflectance measurements from 200-850 nm are performed. Fig. 1 shows the Reflectance of the two samples S1 (20 sccm 1 hr) and S2 (30 sccm 1 hr). The percentage of reflectance of sample 1 and 2 is around 5 % to 12 %. Less reflectance per cent may be due to scattering from large number of grains and grain boundaries present in the MoO<sub>3</sub> samples.

Sample 1 reflectance is slightly less as compare to sample S2. It might be due to high grain boundary density as analysed by XRD and SEM sections. In the reflectance, interference fringes are observed and the thickness of MoO<sub>3</sub> films is determined from fringe separation in the wavenumber scale. The determined thickness of MoO<sub>3</sub> films was 0.5 μm and 1.6 μm for S1 and S2 respectively. The optical absorption of the films is in the range of ~3.25 eV. The optical absorption of MoO<sub>3</sub> films seems to be very close but slightly less than actual bandgap (~3.3eV)<sup>22</sup> of the materials. The less value is due to a slight stoichiometric variation of Mo and O in MoO<sub>3</sub> formation. The thickness of the film in sample S2 determined by the FESEM image is very well matched with thickness determined by UV-visible reflectance. Whereas in sample S1 the thickness determined by reflectance fringes match only from the surface to the first interface of the sample.

The two-layer in sample 1 observed by FESEM images is also seen as the two different phases from XRD. By SEM image upper layer is the orthorhombic α-MoO<sub>3</sub> and other layers may be the oxygen-deficient molybdenum oxide phase. While in sample-2 two-phase of α-MoO<sub>3</sub> and oxygen-deficient MoO<sub>3</sub> phase is present in the whole film therefore large cracks are observed. Since the binding energy of Mo and O in these two phases is different therefore observed cracks from SEM images are large. It is evident from XRD, Raman and SEM images after annealing under Oxygen environment low oxygen and argon flow (20 sccm) films is still oxygen-deficient (sample S1) while high oxygen and argon flow ((30 sccm) film (sample S2) shows the relatively less oxygen deficient.

Further, electrical characterizations of the MoO<sub>3</sub> films are studied by utilizing Au/MoO<sub>3</sub>/Si/Au structure. Figure 5(a) shows the electrical setup for I-V measurement for the Au/MoO<sub>3</sub>/Si/Au structure. For electrical contacts, gold (Au) was deposited on the top of the MoO<sub>3</sub> film 60 nm thick Au electrodes (diameter~ 0.6 mm) by shadow masking and the backside at room temperature by thermal evaporation.

Figure 5(b) shows the J-E characteristics for sample 1 and sample 2. The films are showing Schottky diode characteristics. The reverse leakage current density of sample S2 is found to be ~1x10<sup>-4</sup> mA/cm<sup>2</sup> (high) as compare to sample S1 (~1x10<sup>-6</sup> mA/cm<sup>2</sup>). The high leakage current density of sample 2 is due to large cracks observed in the film and also the excess of oxygen ion vacancies in the MoO<sub>3</sub> films. While low leakage current

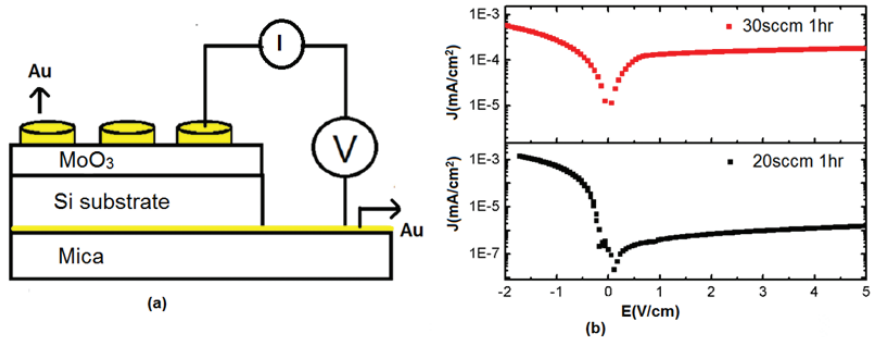


Figure 5. (a) Electrical characterisation setup and (b) J-E characteristics of MoO<sub>3</sub> thin films.

density in sample S1 is due to large and small grains of the films. These MoO<sub>3</sub> thin films can be utilised for gas sensing applications<sup>24</sup>.

#### 4. CONCLUSIONS

The MoO<sub>3</sub> thin films have been successfully deposited on Si substrate by reactive RF magnetron sputtering by varying Ar and O<sub>2</sub> flow (20 sccm and 30 sccm) with 1 h deposition duration with ex-situ annealing in oxygen environment at 500 °C for 4 h. The deposited thin films were found to be a polycrystalline orthorhombic α-MoO<sub>3</sub> phase with preferred orientations along <021> and <110> direction with deficient oxygen MoO<sub>3</sub> films. MoO<sub>3</sub> films grain size varies from 200-400 nm for determined by FESEM. Layer thickness determined by reflectance is very well matched with the cross-sectional FESEM images. The reverse leakage current density of 30 sccm 1-hr sample is large (~1x10<sup>-4</sup> mA/cm<sup>2</sup>) as compare to 20 sccm 1-hr sample (~1x10<sup>-6</sup> mA/cm<sup>2</sup>). These thin MoO<sub>3</sub> films may show a potential candidate for resistive random access memory (ReRAM) and gas sensing applications.

#### REFERENCES

- Dong, W; Ly, Y.; Xiao, L.; Fan, Y.; Zhang, N. & Liu, X. Bifunctional MoO<sub>3</sub>-WO<sub>3</sub>/Ag/MoO<sub>3</sub>-WO<sub>3</sub> Films for Efficient ITO-free electrochromic devices. *ACS Appl. Mat.Interfaces*, 2016, **8**(49), 33842. doi: 10.1021/acsami.6b12346
- Munasinghe, H. M. M.; Dario, A.; Nicola, Z.; Gunawardhana, P.N. & Comini, E. Gold functionalized MoO<sub>3</sub> nano flakes for gas sensing applications. *Sensors Actuators B: Chemical*, 2018, **269**, 331-339. doi: 10.1016/j.snb.2018.04.124
- Kim, W-S; Kim, H-C; & Hong, S-H, Gas sensing properties of MoO<sub>3</sub> nanoparticles synthesized by solvothermal method. *J. Nanoparticle Res.*, 2010, **12**,1889-96. doi: 10.1007/s11051-009-9751-6
- Riley, L.A.; Lee, S.H.; Gedvilias, L. & Dillon, A.C. Optimization of MoO<sub>3</sub> nanoparticles as negative-electrode material in high-energy lithium ion batteries. *J. Power Sources*, 2010, **195**, 588. doi: 10.1016/j.jpowsour.2009.08.013
- Zhou, J; Song, J; Li, H; Feng, X; Huang, Z; Chen, S; Ma, Y; Wanga, L & Yan, X. The synthesis of shape-controlled

- $\alpha$ -MoO<sub>3</sub>/graphene nanocomposites for high performance supercapacitors. *New J. Chem.*, 2015, **39**, 8780.  
doi: 10.1039/C5NJ01722J
6. Sarkar, A.; Ashraf, T.; Grafeneder, W. & Koch, R. Interface structure and composition of MoO<sub>3</sub>/GaAs(001). *J. Phys.: Condens. Matter*, 2018, **30**, 155001.  
doi: 10.1088/1361-648X/aab391
  7. Mohamed, S.H.; Kappertz, O.; Ngaruiya, J.M.; Leervad, Pedersen T.P.; Drese, R. & Wuttig M., Correlation between structure, stress and optical properties in direct current sputtered molybdenum oxide films. *Thin Solid Films*, 2003, **429**, 135-143.  
doi: 10.1016/S0040-6090(03)00068-3
  8. Uthanna, S.; Nirupama, V. & Pierson, J.F. Substrate temperature influenced structural, electrical and optical properties of dc magnetron sputtered MoO<sub>3</sub> films. *Appl. Surf. Sci.*, 2010, **256**, 3133–3137.  
doi: 10.1016/j.apsusc.2009.11.086
  9. Altman, E.I.; Droubay, T. & Chambers, S.A. Growth of MoO<sub>3</sub> films by oxygen plasma assisted molecular beam epitaxy. *Thin Solid Films*, 2002, **414**, 205-215.  
doi: 10.1016/S0040-6090(02)00487-X
  10. Bhosle, V.; Tiwari, A. & Narayan, J. Epitaxial growth and properties of MoO<sub>x</sub>(2<x<2.75)MoO<sub>x</sub>(2<x<2.75) films. *J. Appl. Phys.*, 2005, **97**, 083539.  
doi: 10.1063/1.1868852
  11. Aoki, T.; Matsushima, T.; Mushihiro, K.; Suzuki, A. & Okuda M., Optical recording characteristics of molybdenum oxide films prepared by pulsed laser deposition method. *Thin Solid Films*, 2008, **517**, 1482. <http://dx.doi.org/10.1016/j.tsf.2008.09.060>
  12. Liu, X.; Yi, S.; Wang, C.; Wang, C. & Gao, Y., Electronic structure evolution and energy level alignment at C<sub>60</sub>/4,4'-cyclohexylidenebis[N,N-bis(4-methylphenyl)benzenamine]/MoO<sub>x</sub>/indium tin oxide interfaces. *J. Appl. Phys.*, 2014, **115**, 163708.  
doi: 10.1063/1.4873959
  13. Hosono, K.; Matsubara, I; Murayama, N; Woosuck, S. & Izu N. Synthesis of Polypyrrole/MoO<sub>3</sub> hybrid thin films and their volatile organic compound gas-sensing properties. *Chem. Mater.*, 2005, **17**, 349.  
doi: 10.1021/cm0492641
  14. Bouzidi, A.; Benramdane, N.; Derraz, H.T.; Mathieu, C.; Khelifa, B. & Desfeux, R., Effect of substrate temperature on the structural and optical properties of MoO<sub>3</sub> thin films prepared by spray pyrolysis technique. *Mater. Sci. Eng. B* (2003), **97**, 5-8.  
doi: 10.1016/S0921-5107(02)00385-9
  15. Hsu, C.S.; Chan, C.C.; Huang, H.T.; Peng, C.H. & Hsu, W.C. Electrochromic properties of nanocrystalline MoO<sub>3</sub> thin films. *Thin Solid Films*, 2008, **516**, 4839-4844.  
doi: 10.1016/j.tsf.2007.09.019
  16. Arfaoui, A.; Touihri, S.; Mhamdi, A.; Labidi A. & Manoubi, T. Structural, morphological, gas sensing and photocatalytic characterization of MoO<sub>3</sub> and WO<sub>3</sub> thin films prepared by the thermal vacuum evaporation technique. *Appl. Surf. Sci.*, 2015, **357**, 1089-1096.  
doi: 10.1016/j.apsusc.2015.09.124
  17. Touihri, S.; Arfaoui, A.; Tarchouna, Y.; Labidi, A.; Amlouk, M. & Bernede, J.C., Annealing effect on physical properties of evaporated molybdenum oxide thin films for ethanol sensing. *Appl. Surf. Sci.*, 2017, **394**, 414-424.  
doi: 10.1016/j.apsusc.2016.10.139
  18. Wang, X.; Cui, W.; Chen, M. & Xu, Q. Supercritical CO<sub>2</sub>-assisted Phase Transformation from Orthorhombic to Hexagonal MoO<sub>3</sub>. *Materials Letters*, 2017, **201**, 129–132.  
doi: 10.1007/s40094-014-0161-5
  19. Hojabri, A.; Hajakbari, F. & Meibod, A. E. Multiphase of MoO<sub>3</sub> Structural and optical properties of nanocrystalline  $\alpha$ -MoO<sub>3</sub> thin films prepared at different annealing temperatures. *J. Theorm. Appl. Phys.*, 2015, **9**, 67–73.  
doi: 10.1007/s40094-014-0161-5
  20. Pandey, A.; Dutta, S.; Prakash, R; Dalal, S.; Raman, R.; Kapoor, A. K. & Kaur, D., Growth and evolution of residual stress of AlN films on silicon (100) wafer. *Mater. Sci. Semi. Process*, 2016, **52**, 16-23.  
doi: 10.1016/j.mssp.2016.05.004
  21. Pandey, A.; Kaushik J.; Dutta, S.; Kapoor, A. K. & Kaur, D. Electrical and structural characteristics of sputtered c-oriented AlN thin films on Si (100) and Si (110) substrates. *Thin Solid Films*, 2018, **666**, 143-149.  
doi: 10.1016/j.tsf.2018.09.016
  22. Windom, B.C.; Sawyer, G. & Hahn, D.W. A Raman Spectroscopic Study of MoS<sub>2</sub> and MoO<sub>3</sub>: Applications to tribological systems. *Tribol Lett.*, 2011, **42**, 301–310.  
doi: 10.1007/s11249-011-9774-x
  23. Seguin, L.; Figlarz, M.; Cavagnat, I.R. & Lasskgues, J.-C. Infrared and Raman spectra of MoO<sub>3</sub>, molybdenum trioxides and MoO. xH<sub>2</sub>O molybdenum trioxide hydrates. *Spectrochimica Acta Part A*. 1995, **51**, 1323-1333.  
doi: 10.1016/0584-8539(94)00247-9
  24. Dwivedi, P.; Dhanekar, S. & Das, S. Synthesis of  $\alpha$ -MoO<sub>3</sub> nano-flakes by dry oxidation of RF sputtered Mo thin films and their application in gas sensing. *Semicond. Sci. Technol.*, 2016, **31**, 115010.  
doi: 10.1088/0268-1242/31/11/115010

## ACKNOWLEDGMENTS

The authors would like to thank Director SSPL for her continuous support and kind permission to publish this paper. Help from other colleagues is also acknowledged.

## CONTRIBUTORS

**Dr Akhilesh Pandey** received MSc from Lucknow University, UP and PhD from IIT Roorkee. Presently working as Scientist 'E' in DRDO-Solid State Physics Laboratory, Delhi. His expertise in thin films and device structures characterisation of single-crystal materials, epitaxial layers, multilayer structures. In the current study, he has carried out the complete experimental characterisation work, validated the results, write up, and reviewed the work.

**Ms Anuska Dhaka** received her BTech from Panjab Engineering College, Chandigarh. She did her research internship at DRDO-Solid State Physics Laboratory, Delhi during January 2019-July 2019.

In the current study, she has contributed to the material characterisation experiments and analysis in the present work.

**Dr Chandni Kumari** has completed PhD from IIT Jodhpur. She is currently working on multifunctional materials, focusing on Zinc Oxide and Bismuth Ferrite. Her research area focuses on material synthesis, characterisation, and device applications. The devices which she focuses on RRAM, LED, UV detectors, and chemical and biological sensors.

In the current study, she has grown the MoO<sub>3</sub> thin films on Si(100) substrates by RF magnetron sputtering.

**Dr Janesh Kaushik** received his PhD from IIT Delhi. Presently working as Scientist E in the DRDO-Solid State Physics Laboratory, Delhi. His current research interests are: Device modeling of III-Nitride high frequency and high power devices and electrical characterisation of III-Nitride semiconductor device structures.

In the current study, He is responsible for measurement and analysis of the electrical characterisation of MoO<sub>3</sub> thin films on Si(100) substrates.

**Mr Aman Arora** obtained his ME (Industrial Materials and Metallurgy) from Panjab Engineering College, Chandigarh. Presently working as Scientist E in DRDO-Solid State Physics Laboratory, Delhi. His current research interests are Characterisation of semiconductor material by Electron microscopic techniques.

In the current study, He contributed in the measurement and analysis of planner and cross-sectional FESEM image of MoO<sub>3</sub> thin films on Si(100) substrates.

**Dr Shankar Dutta** received his PhD (MEMS Technology) from IIT Delhi. Presently working as Scientist E in the DRDO-Solid State Physics Laboratory, Delhi. His current research interests are: modeling of MEMS devices; Semiconductor processing; silicon micromachining; residual stress and other integration issues of novel materials with MEMS structures.

In the current study, he has contributed in reviewing the results and overall content of the manuscript.

**Prof. Ambesh Dixit** completed his PhD from Wayne State University (WSU), Detroit, Michigan, USA. Presently working as a Professor at the Indian Institute of Technology, Jodhpur. His current research interests are growth and characterisation of nanostructured materials for alternative energy (both solar photovoltaic and solar thermal) generation and storage electronic materials for multistage memory devices.

In the current study, he has contributed in reviewing the results and overall content of the manuscript. He reviewed the incremental work and provided various valuable inputs.

**Dr R. Raman** has completed his PhD from IIT Madras, Chennai. Presently serving as Scientist-G in DRDO-Solid State Physics Laboratory, Delhi. His current research interests are the Optical characterisation of semiconductor materials and device structures.

In the current study, he has reviewed the work, validated the results, continuously provided the guidance and given many valuable inputs.